Inelastic neutron scattering from solid ^{36}Ar †

Y. Fujii,* N. A. Lurie,‡ R. Pynn, and G. Shirane
Brookhaven National Laboratory, Upton, New York 11973
(Received 25 June 1974)

The phonon dispersion relations of ^{36}Ar have been measured in the [100], [110], and [111] symmetry directions at 10 K using a triple-axis neutron spectrometer. A comparison of the measured dispersion curves and the best available theoretical calculations based on the Bobetic-Barker (BB) potential shows small systematic discrepancies for the [100]L, [110]T_2, [110]L, and [111]L branches. Otherwise the agreement between experiment and theory is remarkably good. The data are well described by several harmonic Born–von Kármán models the most general of which (a three-neighbor general-force model with nine parameters) has been used to deduce values of zero-sound elastic constants. At 10 K (lattice constant $a = 5.313 \pm 0.002$ Å), these are $c_{11} = (424 \pm 5)\times 10^8$, $c_{12} = (239 \pm 5)\times 10^8$, and $c_{44} = (225 \pm 1)\times 10^8$ dyn cm^{-2} which imply a deviation from the Cauchy relation with $\delta = -0.06 \pm 0.02$. From the energies of phonons of small wave vector measured just below the melting point at 82 K ($a = 5.463 \pm 0.002$ Å), the zero-sound elastic constants were determined to be $c_{11} = (248 \pm 6)\times 10^8$, $c_{12} = (153 \pm 5)\times 10^8$, and $c_{44} = (124 \pm 4)\times 10^8$ dyn cm^{-2} ($\delta = -0.19 \pm 0.04$). In both the 10- and 82-K measurements, particular care has been taken to remove the systematic errors introduced by finite instrumental resolution. The measured elastic constants have been compared with several calculations and with results obtained from ultrasonic and Brillouin scattering experiments. Calculations of elastic constants based on the BB potential with the Axilrod-Teller three-body interactions are in good agreement with our data at both temperatures. The energies of some typical phonons have been measured at temperatures of 10, 35, 55, and 75 K. In the only case in which these measurements can be compared with an existing calculation (the [100]T mode at $\zeta = 0.4$), our results show a slightly larger shift of the phonon energy than that computed by Klein *et al.* from the BB potential.

I. INTRODUCTION

Since the first neutron scattering measurements of phonon energies of rare-gas crystals were made by Daniels *et al.*[1] with Kr in 1967, many groups have performed similar measurements with related materials. Recent advances in the understanding of interatomic potentials in rare-gas solids have demanded an increased accuracy in the scattering experiments from which the phonon energies are determined. For this reason, the Brookhaven group has made extensive and precise measurements of phonon dispersion curves and zero-sound elastic constants of He,[2–5] Ne,[6,7] Kr,[1,8,9] and Xe.[10–12] The present work with ^{36}Ar represents a continuation of these studies.

A considerable amount of experimental and theoretical work has been done with Ar. However, natural Ar, consisting of 99.6% ^{40}Ar, 0.3% ^{36}Ar, and 0.1% ^{38}Ar, is an unfavorable material for many neutron measurements because it has a small coherent cross section ($\sigma_{coh} = 0.40$ b) and an appreciable incoherent cross section ($\sigma_{incoh} = 0.25$ b). Thus, Egger *et al.*[13] who, in 1968, measured phonon energies in natural Ar had to use a large (45-cm^3) crystal in order to partially overcome these difficulties. Even so, the data reported by these authors in the large-wave-vector region were, as a result of the substantial incoherent background, not particularly accurate. In contrast to natural Ar, the ^{36}Ar isotope has an unusually large coherent cross section ($\sigma_{coh} = 74$ b). For this reason, Batchelder *et al.*[14] were able to measure phonon energies at 4 K with moderate accuracy using a 0.25-cm^3 crystal of ^{36}Ar. Nevertheless, the experimental situation is still far from well defined; neither set of measurements reported thus far is complete and there is considerable discrepancy between the measurements in certain symmetry directions.

In spite of these inadequacies, the experimental results for Ar have stimulated theoretical investigation of the lattice dynamics of this material. Goldman *et al.*[15] and Niklasson[16] have both used the Lennard-Jones (LJ) potentials to compute phonon energies. More realistic computations based on the Bobetic-Barker (BB) potential and including the Axilrod-Teller three-body interactions have been carried out by Barker *et al.*[17] and have yielded reasonable agreement with the available measurements. Unfortunately, however, the existing data are not of sufficient accuracy to provide a sensitive test of the BB potential.

The temperature dependence of phonon energies provides a further useful test of theoretical models of interatomic forces. In 1971, Batchelder *et al.*[18] measured such temperature dependences for pho-

nons with wave vectors in the [100] direction. These authors compared their results with the calculations of Horton and Leech[19] and with those of Horton *et al.*[20] but neither theory agreed well with experiment. Phonon energy shifts calculated from the BB potential by Klein *et al.*[21] also disagreed with the data. For this reason, it seemed desirable to remeasure the temperature dependences of the energies of some typical phonons both as a check on earlier experimental work and as a stimulus to further theoretical considerations.

Another test of the theoretical models alluded to above is the calculation of elastic constants. In particular, the deviation from the Cauchy relation may provide information about the importance of many-body forces. Measurements of first-sound elastic constants have been made with ultrasonic techniques by Keeler and Batchelder.[22] Brillouin scattering measurements have been performed by Meixner *et al.*[23,24] and more recently by Gewurtz *et al.*[25] These measurements have been compared with varying success to a multitude of calculations which differ in their choice of interatomic potential. It has not been possible on the basis of the elastic constant data to discriminate uniquely among these potentials. Zero-sound elastic constants have been obtained by Dorner and Egger[26] from a neutron scattering experiment with natural Ar. However these results are not sufficiently reliable to allow a detailed comparison to be made with existing calculations. For this reason such measurements, made at 10 and 82 K, are reported in this paper. Particular care has been taken to remove the instrumental inaccuracies which plague neutron measurements of this type.

In Sec. II, a brief description of the method used to grow our ^{36}Ar crystal is given. Experimental details of the neutron scattering experiments and descriptions of the procedures used in the data analysis and correction are given in Sec. III. Section IV is divided into three parts; in the first part, complete dispersion curves obtained at 10 K along the three symmetry directions are presented and analyzed on the basis of several Born–von Kármán models. From these models zero-sound elastic constants and various thermodynamic quantities have been obtained. In the second part of Sec. IV, zero-sound elastic constants obtained from the initial slopes of phonon dispersion curves at 10 and 82 K are presented. Finally, the last part of Sec. IV presents measurements of the temperature dependence of the energy and linewidth of some typical phonons. The concluding section of the paper (Sec. V) is devoted to a comparison of the present results with various theoretical calculations and, where appropriate, with the results obtained with ultrasonic and Brillouin scattering experiments.

II. CRYSTAL GROWTH

A single crystal of ^{36}Ar was grown from the melt by a technique similar to that previously employed for Kr[9] and Xe.[10] A cylindrical sample capsule 6 mm in diameter, 25 mm in height, and wall thicknesses of 0.05 mm was constructed from Kapton (polypyromelitimide) and mounted in a variable-temperature cryostat with the cylinder axis of the capsule vertical. The top and bottom of the capsule were each capped with copper and a stainless-steel tube was brazed in the upper cap to allow gaseous ^{36}Ar to be fed into the capsule. A heater and a calibrated platinum resistance thermometer were also attached to the upper cap. The heater allowed a temperature gradient to be maintained along the axis of the sample capsule during crystal growth. In order to reduce temperature gradients in the sample after the crystal had been grown, the top and bottom caps of the capsule were connected by a copper wire. Measurement of the sample temperature was made with either platinum or germanium resistance thermometers, both of which had been previously calibrated and which were mounted in the copper block of the cryostat. This block was in contact with the lower cap of the sample capsule and its temperature could be maintained to within ± 0.005 K for long periods. Visual inspection of the encapsulated sample was facilitated by the presence of small windows in the cryostat.

^{36}Ar gas of 99.9% purity (Monsanto Research Corp.) was condensed into the sample cell until the latter was filled with liquid. Starting with the base of the cell at 84.5 K and the top at 87.5 K, the temperature was continuously lowered at the rate of 1 K/day with the 3-K temperature differential between the top and bottom of the cell maintained throughout. When the temperature of the base had reached 82 K (melting point = 83.7 K), the capsule heater was turned off and a uniform sample temperature of 82 K was achieved after about 8 h. At this temperature the sample was annealed for about 12 h.

Polaroid pictures of a neutron beam Bragg reflected from the sample showed the latter to be a large single crystal which filled the bulk of the sample container. The crystal was found to have grown with a [110] direction at about 10° to the cylinder axis of the cell. Thus both (110) and (112) zones could be used for phonon measurements without requiring the cryostat to be tilted through alarming angles. In these two zones all phonon branches along the three symmetry directions [100], [110], and [111] could be measured. The mosaic of the crystal at 82 K, determined in the usual way with a perfect germanium crystal, was found to be 7 min [full width at half-maximum (FWHM)].

To facilitate the cooling of the sample the container was connected to a vacuum pump and the surface of the crystal was allowed to sublimate, thereby freeing the crystal from the cell walls. This pumping procedure increased the crystal mosaic from 7 to 12 min. Cooling to 10 K further broadened the mosaic to 21 min. Since further cooling would probably have resulted in an increase in mosaic spread it was decided that measurements of phonon energies at low temperature should be made at 10 K. After measurements of phonon energies at this temperature had been completed the crystal was inadvertently further cooled and its mosaic was thereby increased to 34 min. Subsequent heating of the crystal, required during measurements of the temperature dependence of some phonon energies, resulted in still further changes in mosaic width. Values of 30, 35, and 24 min were observed at 35, 55, and 75 K, respectively. The low value at 75 K arose because, at this temperature, the crystal split into two parts of which the usable portion had a mosaic of 24 min. In addition to these fluctuations in mosaic spread the angular distribution of mosaic grains became somewhat asymmetric as the crystal was heated.

III. EXPERIMENTAL DETAILS

Measurements of phonon energies were performed with the triple-axis spectrometer at the Brookhaven High Flux Beam Reactor. Incident neutron energies of 5.0, 13.7, and 30.5 meV were used at various stages of the experiment. Monochromator and analyzer crystals were of pyrolytic graphite; the former was vertically bent while the latter was planar. Horizontal collimations (in-pile, monochromator-sample, sample-analyzer, and analyzer-detector) were either 20 or 40 min. Higher-order contamination of the incident neutron beam was removed by a graphite filter or, for 5.0-meV incident neutrons, by a cooled beryllium filter. During the measurements of phonon energies the spectrometer was operated entirely in the constant-Q mode. Many of the phonons were measured at equivalent points in reciprocal space and some measurements were performed with more than one value for the incident energy. In addition, some phonons, particularly those of small wave vector, were observed both via neutron-energy-loss and neutron-energy-gain processes. While the energy-gain measurements were straightforward at 82 K they were much less tractable at 10 K as a result of the small occupation number for phonon states at this temperature. In Fig. 1 some "typical" phonon profiles, which serve to demonstrate the quality of our data, are displayed.

All experimental data were corrected for the effects of the finite resolution of the spectrometer. In the procedure adopted each constant-Q scan was first fitted to the sum of one or two Gaussian functions and a linearly varying background. From the positions of the Gaussians, initial estimates of all phonon energies were obtained and fitted to a force-constant model which involved general forces extending to third neighbors. The force constants so obtained were used in conjunction with a computer program[27] to generate an expected, resolution-broadened profile for each constant-Q scan. This computer generated profile was fitted, in the manner described above, to sum of Gaussian and background terms. Each phonon profile could then be associated with three different energies; the initial experimental estimate of the phonon energy (ω_E), the phonon energy predicted by the fitted force constants (ω_0), and the phonon energy obtained from the computer-generated constant-Q profiles (ω). In order to correct ω_E for the effects of finite instrumental resolution, the quantity $(\omega_0 - \omega)$ was added to ω_E. This correction was found to be particularly important in the small wave vector region and at zone boundaries; in the former case correction $(\omega_0 - \omega)$ of order 5% of ω_E were not uncommon.

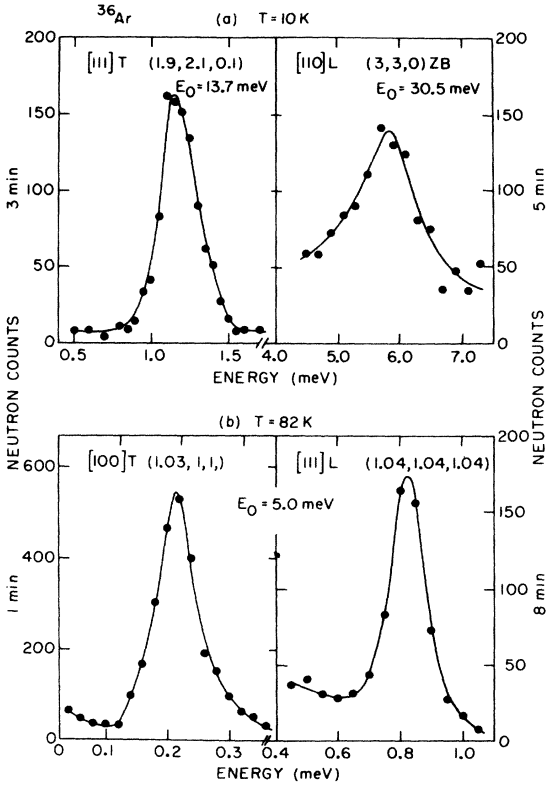

FIG. 1. Typical phonon scans of (a) [111]T and [110]L modes at 10 K and (b) [100]T and [111]L modes at 82 K.

TABLE I. Phonon energies of solid ^{36}Ar at temperatures of 10 and 82 K (in mev).

[ζ00]

	T		L	
ζ	10 K	82 K	10 K	82 K
0.02	···	0.158 ± 0.004	···	···
0.03	···	0.216 ± 0.006	···	···
0.04	···	0.285 ± 0.004	···	0.41 ± 0.02
0.05	···	0.340 ± 0.004	···	0.51 ± 0.01
0.06	···	0.410 ± 0.004	···	0.61 ± 0.02
0.07	···	0.473 ± 0.004	···	0.72 ± 0.01
0.08	0.739 ± 0.006	0.532 ± 0.004	1.01 ± 0.02	0.81 ± 0.02
0.09	0.80 ± 0.02	0.600 ± 0.006	···	···
0.10	0.90 ± 0.01	0.664 ± 0.006	···	···
0.12	1.06 ± 0.02	···	···	···
0.15	1.35 ± 0.01	1.09 ± 0.01	1.87 ± 0.06	1.62 ± 0.02
0.20	1.79 ± 0.01	1.41 ± 0.02	2.50 ± 0.02	2.05 ± 0.02
0.25	2.23 ± 0.01	1.74 ± 0.02	3.04 ± 0.02	2.61 ± 0.04
0.30	2.67 ± 0.01	2.09 ± 0.05	3.65 ± 0.02	···
0.40	3.46 ± 0.01	···	4.79 ± 0.02	···
0.50	4.18 ± 0.01	···	5.85 ± 0.02	···
0.60	4.76 ± 0.01	···	6.84 ± 0.08	···
0.70	5.25 ± 0.01	···	7.44 ± 0.07	···
0.80	5.61 ± 0.02	···	7.97 ± 0.06	···
0.90	5.82 ± 0.02	···	8.27 ± 0.06	···
0.95	5.88 ± 0.02	···	···	···
1.00	···	···	8.32 ± 0.06	···

[ζζ0]

	T_1		T_2		L	
ζ	10 K	82 K	10 K	82 K	10 K	82 K
0.03	0.259 ± 0.002	···	0.425 ± 0.006	0.307 ± 0.006	···	···
0.04	0.361 ± 0.008	0.233 ± 0.006	···	0.403 ± 0.004	···	0.65 ± 0.01
0.05	0.439 ± 0.006	···	0.670 ± 0.008	0.487 ± 0.004	0.99 ± 0.03	0.80 ± 0.01
0.06	0.517 ± 0.006	0.361 ± 0.004	0.825 ± 0.006	0.594 ± 0.008	1.15 ± 0.03	0.95 ± 0.01
0.07	···	0.421 ± 0.004	0.94 ± 0.01	0.688 ± 0.004	1.43 ± 0.02	···
0.08	0.685 ± 0.006	0.477 ± 0.004	1.068 ± 0.004	0.79 ± 0.01	···	···
0.09	···	0.543 ± 0.006	···	0.880 ± 0.004	···	···
0.10	0.85 ± 0.01	0.604 ± 0.006	1.312 ± 0.006	1.06 ± 0.01	2.02 ± 0.02	1.64 ± 0.02
0.12	1.01 ± 0.01	0.708 ± 0.009	1.57 ± 0.01	···	2.38 ± 0.04	···
0.14	1.18 ± 0.01	0.843 ± 0.008	···	···	2.93 ± 0.02	···
0.15	···	0.89 ± 0.01	1.96 ± 0.01	1.52 ± 0.02	···	2.44 ± 0.02
0.16	1.35 ± 0.01	0.96 ± 0.01	···	···	···	···
0.20	1.65 ± 0.02	1.22 ± 0.02	2.56 ± 0.01	1.98 ± 0.04	3.87 ± 0.04	···
0.25	2.05 ± 0.02	···	···	···	···	···
0.30	2.46 ± 0.03	···	3.78 ± 0.01	···	5.47 ± 0.03	···
0.40	3.24 ± 0.01	···	4.89 ± 0.01	···	6.51 ± 0.08	···
0.50	3.95 ± 0.02	···	5.91 ± 0.02	···	7.48 ± 0.15	···
0.60	4.63 ± 0.02	···	···	···	7.44 ± 0.07	···
0.70	5.24 ± 0.02	···	7.45 ± 0.04	···	7.22 ± 0.06	···
0.80	5.63 ± 0.04	···	8.03 ± 0.06	···	6.55 ± 0.03	···
0.90	5.79 ± 0.12	···	8.27 ± 0.03	···	6.15 ± 0.08	···
0.95	5.95 ± 0.04	···	8.30 ± 0.09	···	···	···
1.00	5.94 ± 0.03	···	8.32 ± 0.06	···	5.94 ± 0.10	···

[ζζζ]

	T		L	
ζ	10K	82 K	10 K	82 K
0.02	···	0.197 ± 0.006	0.51 ± 0.01	0.37 ± 0.02
0.03	0.36 ± 0.01	0.278 ± 0.006	0.78 ± 0.01	0.61 ± 0.01
0.04	0.51 ± 0.01	0.368 ± 0.004	1.05 ± 0.02	0.82 ± 0.01
0.05	0.61 ± 0.01	0.447 ± 0.006	1.28 ± 0.03	1.02 ± 0.01
0.06	0.71 ± 0.02	0.556 ± 0.006	···	1.21 ± 0.03
0.07	···	0.650 ± 0.008	1.82 ± 0.03	···
0.08	0.95 ± 0.01	0.744 ± 0.006	···	···
0.10	1.19 ± 0.02	0.966 ± 0.008	2.54 ± 0.02	2.04 ± 0.03
0.12	1.43 ± 0.01	1.22 ± 0.02	···	···
0.15	1.77 ± 0.02	1.43 ± 0.04	3.99 ± 0.04	3.06 ± 0.05
0.20	2.31 ± 0.01	1.82 ± 0.04	5.05 ± 0.07	4.18 ± 0.08
0.25	2.78 ± 0.02	···	5.96 ± 0.05	···
0.30	3.20 ± 0.02	···	6.83 ± 0.06	···
0.40	3.81 ± 0.02	···	8.07 ± 0.06	···
0.45	4.05 ± 0.03	···	···	···
0.50	3.97 ± 0.04	···	8.35 ± 0.10	···

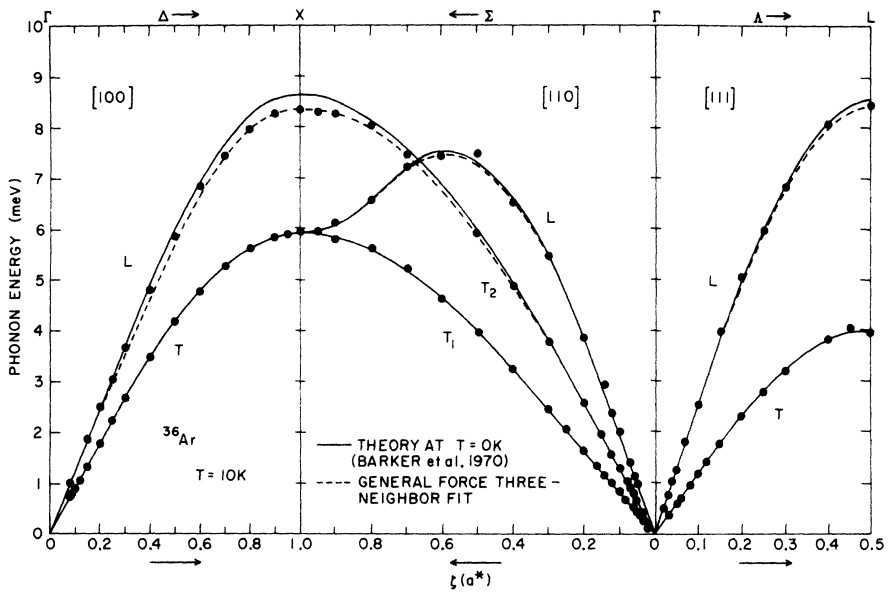

FIG. 2. Phonon-dispersion relations of ^{36}Ar along the three symmetry directions. The solid circles are the resolution-corrected measurements at 10 K. The dashed line is a general-force three-neighbor model fitted to the data and the solid line represents a theoretical calculation at 0 K based on the BB potential by Barker *et al.* (Ref. 17).

IV. RESULTS AND ANALYSIS

A. Phonon dispersion relation at 10 K

Phonon energies, measured at 10 and 82 K and corrected for the effects of finite instrumental resolution, are displayed in Table I. Phonon wave vectors q are given in the table in terms of the reduced unit ζ, where $\zeta = q(a/2\pi)$ and a is the measured lattice constant (at 10 K, $a = 5.313 \pm 0.002$ Å). The uncertainties in the phonon energies which are quoted in Table I are twice those which are obtained when Gaussian curves are fitted to the observed phonon profiles (cf. Sec. III). This escalation of the uncertainties is intended to account for the small errors which inevitably arise in setting and reading the angles which define a spectrometer configuration. While such errors are systematic for a particular constant-Q scan they are, to a good approximation, randomly distributed over a large set of such scans. The escalation factor of 2 has been chosen to ensure that the force constant model (either of models 2 and 3 described below) which gives the best fit to the data yields a value of unity for the χ^2 [cf. Eq. (1)] obtained in a least-square fit. The data at 10 K displayed in Table I are plotted in Fig. 2. Note that the uncertainties in the phonon energies are less than the size of plotted symbols in this figure.

A program developed by Svensson *et al.*[28] was used to fit several Born–von Kármán models to the 10-K data. To obtain the force constants of these models the quantity

$$\chi^2 = \frac{1}{N-P} \sum_{i=1}^{N} \left(\frac{\omega_{io}^2 - \omega_{ic}^2}{2\sigma_i \omega_{io}} \right)^2 \qquad (1)$$

was minimized in the usual least-square manner. In Eq. (1), ω_{io} and ω_{ic} are the observed and calculated energies of the ith phonon, σ_i is an estimate of the uncertainty in ω_{io} (cf. Table I) and $N-P$ is the number of fitted phonons minus the number of independent force constants. Three different models were fitted to the data. Models 1 and 2 involved, respectively, axially symmetric and general force constants between an atom and its first, second and third neighbors. Model 3 was an eight-neighbor model in which general force constants were used to describe interactions extending to third neighbors. The force constants for the remaining five neighbors were obtained from the van der Waals potential $-C/r^6$ with the constant C ($= 0.630 \times 10^{-10}$ erg Å^6) taken from the work of Starkschall and Gordon.[29] The force constants obtained with these three models are summarized in Table II. Models 2 and 3 give nearly equal values of χ^2 while both of these models are in slightly better agreement with the data than is model 1. On the scale of Fig. 2 however the dispersion curves obtained from the three models cannot be distinguished from one another. The models yield the dashed curves in Fig. 2. Solid curves in this figure represent the theoretical zero-temperature calculations of Barker *et al.*[17] which were based on the BB potential.

Force constants obtained from model 2 were used, in conjunction with the program of Gilat and Raubenheimer,[30] to calculate the phonon density of states $g(\omega)$. The result of this calculation is shown in Fig. 3 as a histogram with channel width 0.004 meV. From this density of states the specific heat at constant volume C_v was calculated in the

TABLE II. Interatomic force constants (in dyn cm^{-1}) of solid ^{36}Ar at $T=10$ K. Model 1 involves axially symmetric three-neighbor forces; model 2 includes general force extending to third neighbors. Model 3 involves eight neighbors of which the force constants for the first three neighbors have been fitted to general forces and the fourth-to-eighth neighbor interactions are derived from the theoretical van der Waals potential of Ref. 29. The fourth column shows the force constants determined at 4 K from a general force two-neighbor model fitted to the neutron scattering data of Batchelder *et al.* (Ref. 14). [For general forces, symmetry requires $1YY=1XX$, $1YZ=1ZX=0$, $2ZZ=2YY$, $2YZ=2ZX=2XY=0$, $3ZZ=3YY$, and $3XY=3ZX$. For axially symmetric forces, one has additional conditions $\alpha=1XX-1ZZ-1XY$, $\beta=3XX-3YY-3(3YZ)$, $\gamma=2(3XX)-2(3YY)-3(3ZX)$, where $\alpha=\beta=\gamma=0$.]

Force constant	Model 1	Model 2	Model 3	Batchelder *et al.* ($T=4$ K)
$1XX$	608 ± 4	605 ± 5	605 ± 5	604
$1ZZ$	−8 ± 3	5 ± 7	0 ± 7	−7
$1XY$	617 ± 5	633 ± 9	633 ± 9	531
$2XX$	−44 ± 4	−24 ± 11	−24 ± 11	−60
$2YY$	−2 ± 3	−3 ± 4	−1 ± 4	−21
$3XX$	0 ± 2	−5 ± 4	−2 ± 4	···
$3YY$	0 ± 1	0 ± 1	0 ± 1	···
$3YZ$	0 ± 1	0 ± 2	−1 ± 2	···
$3ZX$	0 ± 1	−2 ± 2	−1 ± 2	···
α	0	−32 ± 12	−28 ± 12	80
β	0	−5 ± 5	0 ± 5	···
γ	0	−3 ± 7	−1 ± 7	···

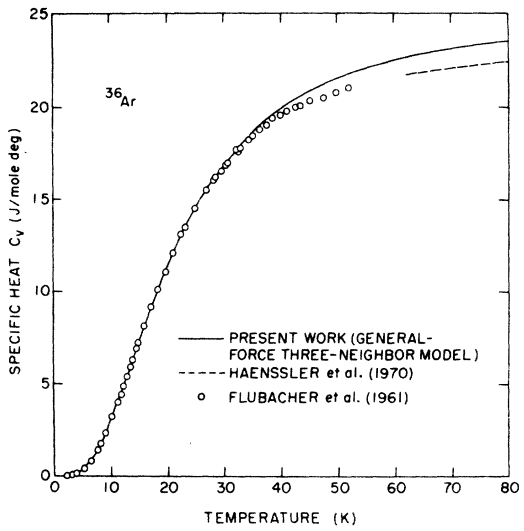

FIG. 4. Specific heat C_v of ^{36}Ar. The solid line is calculated from the phonon density of states in Fig. 3. The open circles have been obtained from the C_p measurements of natural Ar which were made by Flubacher *et al.* (Ref. 31). These results have been corrected to give C_v and converted to ^{36}Ar using the procedure outlined in the text [cf. Eq. (2)]. The dashed line represents the C_v measurement of natural Ar made by Haenssler *et al.* (Ref. 33) which has been converted to ^{36}Ar.

harmonic approximation and this quantity is displayed as the solid curve in Fig. 4. Calorimetric measurements of the constant-pressure specific heat C_p of ^{40}Ar have been made by Flubacher *et al.*[31] The difference between C_p and C_v at any given temperature was interpolated from the work of Beaumont *et al.*[32] and values of C_v were thereby deduced from measured values of C_p. In order to calculate the specific heat $C_v^{36}(T)$ of ^{36}Ar at a temperature T from the specific heat $C_v^{40}(T)$ of ^{40}Ar it was assumed that the same interatomic force constants applied to crystals of each isotope. In this case phonon energies in crystal of the two isotopes differ only by virtue of the difference in atomic mass and one finds that

$$C_v^{40}(T)=C_v^{36}[(\tfrac{40}{36})^{1/2}T]\ . \qquad (2)$$

This equation may be understood by noting that C_v is a function of T/Θ_D (where Θ_D is the Debye temperature) and Θ_D^2 is proportional to the inverse of the atomic mass. Calorimetric measurements corrected according to this procedure are represented by the circular symbols in Fig. 4. The dashed line at the high-temperature end of Fig. 4 has been obtained from the experimental results of Haenssler *et al.*[33]

The calculated specific heat (solid curve in Fig. 4) has been used to determine effective Debye temperatures. These values are represented by the solid line in Fig. 5. The dashed line in this figure shows the Debye temperature obtained from a calculation of the Debye-Waller factor. Also shown in Fig. 5 are a number of values of the Debye temperature at 0 K which have been previously determined either from measured[14,32,34] or calculated[17]

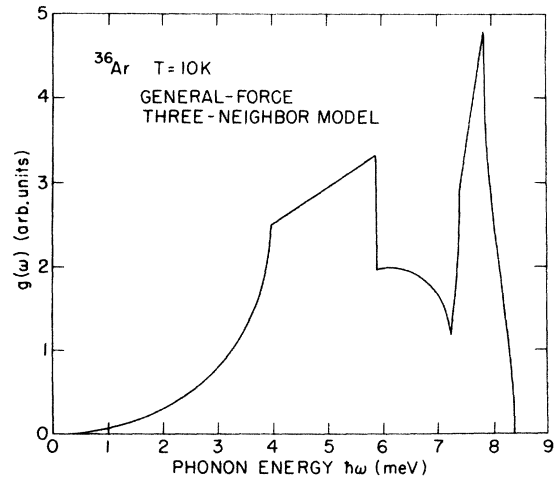

FIG. 3. Phonon density of states of ^{36}Ar at 10 K obtained from a general-force three-neighbor model.

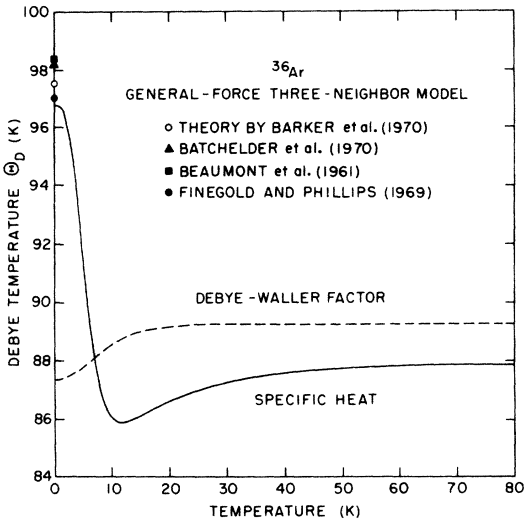

FIG. 5. Debye temperature of ^{36}Ar for the specific heat and for the Debye-Waller factor. At 0 K, earlier experimental (solid symbols) and theoretical (open circle) values for the specific heat are shown. The values obtained for natural Ar have been converted to ^{36}Ar according to the procedure described in the text.

values of C_v. Of these results only those of Batchelder *et al.*[14] were obtained with ^{36}Ar. The remaining results, originally quoted for ^{40}Ar, have been converted to values relevent to ^{36}Ar by making use of the procedure outlined in the sentences which follow Eq. (2).

B. Zero-sound elastic constants at 10 and 82 K

Zero-sound elastic constants may be determined from measured phonon energies by the method of long waves, a procedure which relates elastic constants to the gradient of the phonon dispersion surface at the center of the Brillouin zone. To obtain such gradients one may proceed in one of two ways: (i) A force-constant model may be fitted to some or all of the data and the gradient determined from the force constants; (ii) a polynomial function of the wave vector q may be fitted to the energies of phonons with small q and the gradient determined as the coefficients of the term linear in q. For the data obtained in this experiment, both methods may, in principle, be used at 10 K since complete dispersion curves have been measured. At 82 K, however, measurements could not be made for large values of q because sample anharmonicity caused excessive broadening and lack of definition of phonon profiles. Thus, at 82 K, method (ii) was the only viable alternative.

At 10 K, the force constants of models 1, 2, and 3 (cf. Table II) yield the elastic constants shown in rows (a), (b), and (c) of Table III. Also shown in the latter table are values of the bulk modulus $B_0 = \frac{1}{3}(c_{11} + 2c_{12})$, the elastic anisotropy $A = 2c_{44}/(c_{11} - c_{12})$ and a measure, $\delta = (c_{44} - c_{12})/c_{12}$, of the deviation from the Cauchy relation.

Phonon energies $\hbar\omega$ in the small wave-vector region, measured at 82 K, were represented by the equation[8]

$$\hbar\omega = \epsilon + v_s q + Bq^3 \quad , \tag{3}$$

and the parameters ϵ, v_s, and B were determined for each phonon branch from a least-square-fitting procedure. In order to determine a reliable value of ϵ, phonons measured via neutron-energy-loss and neutron-energy-gain procedures were, in the fitting procedure, given positive and negative energies, respectively. In the absence of systematic errors in the setting of the zero of the energy scale, a value of zero ought to be calculated for the parameter ϵ. In practice, it was found that the fitted value of ϵ was always less than its uncertainty and thus our results are free from this type of systematic error. Sound speeds v_s were calculated for each of the seven acoustic phonon branches in [100], [110], and [111] directions. The elastic constants were then obtained by performing a least-square fit of these constants to the sound speeds. Elastic constants obtained in this manner are displayed in Table III under the heading "sound speed" [row (k)].

Attempts to apply the above sound-speed method to the 10-K data met with difficulties not experienced with the 82-K data. Unfortunately, the relatively large mosaic (21 min) of the 10-K sample (cf. 7 min at 82 K) made it impossible to determine phonon energies at very small wave vectors (cf. Table I). This difference between the experiments at 10 and 82 K is clearly demonstrated in Fig. 6 which displays the data used with the sound-speed method at both temperatures. The 10-K data were, in fact, insufficient to determine adequately the parameters ϵ, v_s, and B for all phonon branches. To circumvent this difficulty ϵ was in all cases set to zero before the fitting procedures described in the previous paragraph were repeated with the 10-K data. Results obtained from this sound-speed method at 10 K are displayed in row (d) of Table III. Evidently these results are in agreement with those cited in rows (a), (b), and (c) of Table III which were obtained from the force-constant models. However for the reasons outlined above sound-speed results at 10 K are the least reliable.

Those rows of Table III not yet described [row (e)–(j) and rows (l)–(q)] give elastic constants which have either been calculated or measured by other authors. Comparison of the various rows of the table is postponed until Sec. V. It is perhaps worth pointing out that, although some of the results given in Table III were originally quoted for ^{40}Ar, the harmonic elastic constants are independent of

TABLE III. Elastic properties of solid Ar at temperatures of 10 and 82 K. The elastic constants c_{ij} and the bulk modulus B_0 are given in units of 10^{9} dyn cm^{-2}: $A = 2c_{44}/(c_{11}-c_{12})$ and $\delta = (c_{44}-c_{12})/c_{12}$ are dimensionless.

$T=10$ K	c_{11}	c_{12}	c_{44}	B_0	A	δ
Present work						
(a) Model 1[a]	425 ± 5	240 ± 5	224 ± 1	302 ± 4	2.42 ± 0.09	−0.07 ± 0.02
(b) Model 2[a]	424 ± 5	239 ± 5	225 ± 1	301 ± 4	2.43 ± 0.09	−0.06 ± 0.02
(c) Model 3[a]	420 ± 5	235 ± 5	225 ± 1	297 ± 4	2.43 ± 0.09	−0.04 ± 0.02
(d) Sound speed[b]	421 ± 8	227 ± 9	217 ± 6	292 ± 7	2.24 ± 0.15	−0.04 ± 0.05
Other experiments						
(e) Neutron($T=4$ K)[c]	411	190	210	264	2.64	0.11
(f) Neutron($T=4$ K)[d]	367 ± 14	174 ± 17	234 ± 11	238 ± 15	2.42 ± 0.30	0.34 ± 0.12
(g) Brillouin ($T=0$ K)[e]	~400	~200	228		1.9	
(h) Ultrasonic[f]	434 ± 11	182 ± 12	161 ± 4	266 ± 9	1.28 ± 0.09	−0.10 ± 0.11
Theories						
(i) Barron and Klein[g] ($T=0$ K)	371	207	215	262	2.62	0.04
(j) Barker *et al.*[h] ($T=0$ K)	416	230	228	293	2.46	−0.01
$T=82$ K	c_{11}	c_{12}	c_{44}	B_0	A	δ
Present work						
(k) Sound speed[b]	248 ± 6	153 ± 5	124 ± 4	181 ± 4	2.61 ± 0.23	−0.19 ± 0.04
Other experiments						
(l) Brillouin[i]	233 ± 8	149 ± 6	117 ± 7	177 ± 7	2.80 ± 0.60	−0.22 ± 0.06
(m) Ultrasonic[f] ($T=80$ K)	270 ± 6	139 ± 10	89 ± 2	183 ± 7	1.36 ± 0.12	−0.36 ± 0.05
Theories						
(n) Holt *et al.*[j] ($T=80$ K)	231	153	120	179	3.1	−0.216
(o) Klein and Murphy[k] ($T=80$ K)	250	163	119	192	2.74	−0.270
(p) Fisher and Watts[l] ($T=80$ K)	244	161	112	189	2.70	−0.304
(q) Gibbons *et al.*[m] ($T=80$ K)	237	157	112	184	2.80	−0.287

[a]See Table II.
[b]Determined by fitting sound speed to the small-wave-vector phonon data.
[c]D. N. Batchelder *et al.* (Ref. 14).
[d]B. Dorner and H. Egger (Ref. 26).
[e]H. Meixner *et al.* (Refs. 23 and 24).
[f]G. L. Keeler and D. N. Batchelder (Ref. 22).
[g]LJ potential (Ref. 35).
[h]BB potential (Ref. 17).
[i]S. Gewurtz *et al.* (Ref. 25).
[j]L-J potential [A. C. Holt, W. G. Hoover, S. G. Gray, and D. R. Shortle, Physica (Utr.) 49, 61 (1970)].
[k]BB potential [M. L. Klein and R. D. Murphy, Phys. Rev. B 6, 2433 (1972)].
[l]Barker-Fisher-Watts potential [R. A. Fisher and R. O. Watts, Molec. Phys. 23, 1051 (1972)].
[m]Parson-Siska-Lee potential [T. G. Gibbons, M. L. Klein, and R. D. Murphy, Chem. Phys. Lett. 18, 325 (1973)].

the isotope used if the interatomic force constants and the lattice constant are unchanged by the substitution of ^{36}Ar for ^{40}Ar. The former assumption is well justified on theoretical grounds and the latter has been verified by comparing the lattice constants measured in our experiment with those quoted by other authors. Anharmonic corrections to the elastic constants are, according to the work of Barron and Klein,[35] expected to be independent of isotopic mass at high temperatures. At low temperatures the expressions of Barker *et al.*[17] indicate that the difference in mass of ^{36}Ar and

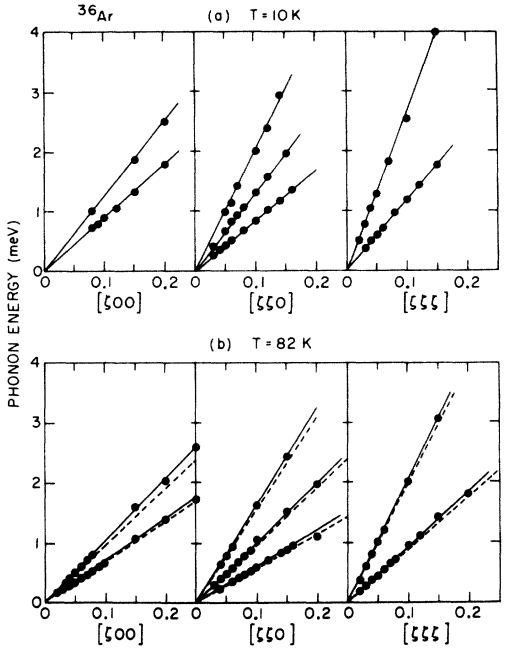

FIG. 6. Resolution-corrected phonon dispersion relations in the small wave vector region of ^{36}Ar at (a) 10 K and (b) 82 K. The solid lines represent a sound speeds fitted to the phonon data and the dashed lines at 82 K are calculated from the first sounds of natural Ar measured in the Brillouin scattering experiments of Gewurtz *et al.* (Ref. 25).

^{40}Ar should lead to a difference of less than 1% in the elastic constants of these two isotopes.

C. Temperature dependence of phonon energies

An attempt has been made to measure the energies and natural linewidth of selected phonons at constant pressure and at temperatures of 10, 35, 55, and 75 K. For this part of the experiment incident neutrons of energy 13.7 meV were used. Horizontal collimations of 40 min (FWHM) were used in the in-pile and analyzer-detector positions while 20-min collimators were placed between monochromator and sample and between sample and analyzer. During this part of experiment the angular distribution of mosaic grains of the crystal changed with temperature in the manner described in Sec. II. For this reason it has been impossible to extract from the data meaningful values of the phonon linewidth and attention has therefore focused on the temperature dependence of phonon energies. An example of the results obtained is displayed in Fig. 7. For the reasons outlined above no quantitative conclusions about sample anharmonicity should be drawn from the variation of the intensity and width of the phonon profile displayed in this figure. However, the energy shifts do provide such information. The correction of data like those displayed in Fig. 7 for the effects of finite instrumental resolution was complicated by the variation of sample mosaic between experiments at different temperatures. To the extent that this variation was known it was included in the resolution calculation according to the method described by Werner and Pynn.[27] Since the energy shifts introduced by finite resolution usually vary slowly both with phonon energy and wave vector, the force-constant model 2 (cf., Table II), which describes the 10-K data, was used to compute these shifts at all temperatures. Thus, the shifts for a given phonon, computed according to the method described in Sec. III, vary with temperature only as a result of the variation of sample mosaic.

Phonon energies, resolution corrected according to the above procedure, are listed in Table IV together with the lattice constants measured during the experiment. Blanks in the table occur for cases in which a phonon profile was too broad and weak to provide a reasonable estimate of the phonon energy. In Table IV, numbers in parentheses represent the percentage shift (defined as $\{\omega(10\text{ K}) - \omega(T)]/\omega(10\text{ K})\}\times 100$) in the energies of phonons. Of the data displayed in Table IV only those for the [100]T mode at $\zeta = 0.4$ are directly comparable with existing measurements or calculations. Results for this case are shown in Fig. 8 together with the measurements of Batchelder *et al.*[14] and the calculated values obtained by Klein *et al.*[21] from the BB potential.

V. DISCUSSION

In Fig. 2 the measured phonon energies of ^{36}Ar are compared with dispersion curves calculated by Barker *et al.*[17] The calculation, performed

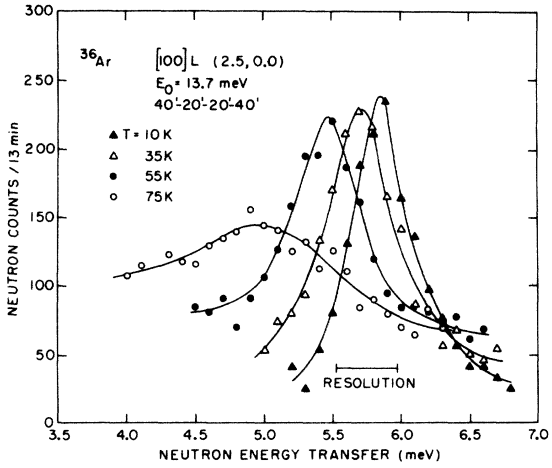

FIG. 7. Measurement of the temperature shift of phonon energy of the [100]L mode with $\zeta = 0.5$.

TABLE IV. Temperature dependence of phonon energies of solid ^{36}Ar (in meV). Relative energy shifts defined by $\{[\omega(10\text{ K}) - \omega(T)]/\omega(10\text{ K})\} \times 100$ are shown in parentheses.

Mode	ζ	$T = 10$ K	35 K	55 K	75 K
[100]T	0.4	3.42 ± 0.01	3.29 ± 0.03 (3.8 ± 1.2)	3.09 ± 0.04 (9.6 ± 1.4)	2.95 ± 0.04 (13.7 ± 1.4)
	0.8	5.61 ± 0.02	5.49 ± 0.02 (2.1 ± 0.7)	...	...
[100]L	0.3	3.63 ± 0.04	3.57 ± 0.02 (1.7 ± 1.6)	3.41 ± 0.04 (6.1 ± 2.1)	3.21 ± 0.03 (11.6 ± 1.8)
	0.5	5.86 ± 0.03	5.70 ± 0.02 (2.7 ± 0.8)	5.46 ± 0.04 (6.8 ± 1.2)	5.02 ± 0.08 (14.3 ± 1.8)
[110]T_2	0.3	3.80 ± 0.01	3.70 ± 0.01 (2.6 ± 0.5)	3.49 ± 0.03 (8.2 ± 1.0)	...
[110]L	0.3	5.39 ± 0.02	5.29 ± 0.03 (1.9 ± 0.9)	5.09 ± 0.04 (5.6 ± 1.0)	...
[111]T	0.2	2.32 ± 0.01	2.22 ± 0.01 (4.3 ± 0.8)	2.07 ± 0.01 (10.8 ± 0.8)	1.91 ± 0.02 (17.7 ± 1.2)
	0.4	3.81 ± 0.02	3.65 ± 0.02 (4.2 ± 1.0)	3.41 ± 0.02 (10.5 ± 1.0)	...
Lattice constant (Å)		5.313 ± 0.002	5.341 ± 0.002	5.383 ± 0.002	5.437 ± 0.002

for ^{36}Ar at 0 K, was based on the BB potential with three-body forces represented by an Axilrod-Teller interaction. As Fig. 2 shows there is some systematic discrepancy between calculation and measurement especially for the high-energy phonons. Some reduction of this discrepancy might be achieved (cf. Table IV) by including the anharmonic effects relevant at 10 K. However such an improvement for the high-energy phonons would have a concomitant adverse effect on the agreement between measured and calculated energies of the low-energy [100]T, [110]T_1, and [111]T branches. Thus one is led to conclude that the BB potential gives good but not perfect agreement with measured phonon energies in ^{36}Ar. This result is reminiscent of that found earlier for Kr.[9]

Of the parameters α, β, and γ listed in Table II for force-constant models 2 and 3 only α is significantly different from zero. Since α measures the departure from centrality of first-neighbor forces one is led to conclude that such noncentral forces are, in Ar, of extremely short range. However, in view of the small value of α and the marginal difference between the quality of the fits obtained with models 1 and 2, even this conclusion must be regarded as somewhat tentative. As Klein *et al.*[21] have shown it is extremely difficult to use the phonon energies of Ar to estimate magnitude of noncentral interactions in this material.

The computed specific heat C_v displayed in Fig. 4 shows good agreement with calorimetric measurements at temperatures less than about 30 K. Although this agreement is gratifying it ought not to be overinterpreted. Barron[36] has shown that, at any temperature T, there is a phonon density of states $g^{\text{eff}}(\omega, T)$ which, if used in conjunction with a quasiharmonic model of lattice vibrations, yields the correct specific heat. However $g^{\text{eff}}(\omega, T)$ is, as a result of sample anharmonicity, not identical to the density of states $g(\omega, T)$ measured in a neutron scattering experiment. Thus the strongest conclusion one may draw from Fig. 4 is that sample anharmonicity does not imply a large difference between $g(\omega, T = 10\text{ K})$ and $g^{\text{eff}}(\omega, T)$ at temperatures below 30 K. At higher temperatures the difference between $g(\omega, T)$ measured at 10 K and the appropriate $g^{\text{eff}}(\omega, T)$ becomes increasingly significant and is reflected in the increasing discrepancy between the solid curve and the open circles in Fig. 4. This discrepancy is not unique to Ar: similar results have been obtained for example in the case of Xe.[12]

Zero-sound elastic constants measured at 4 K in previous neutron experiments are shown in rows (e) and (f) of Table III. Row (e) was obtained by

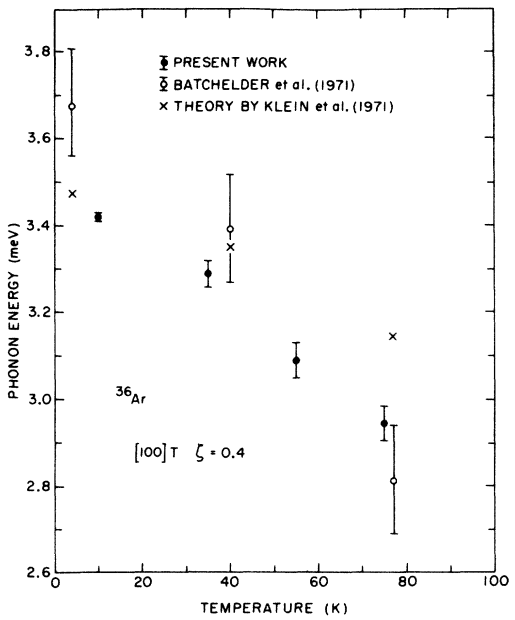

FIG. 8. Temperature dependence of phonon energy of the [100]T mode with $\zeta = 0.4$. The solid circles are the present resolution-corrected data and the open circles are experimental results of Batchelder *et al.* (Ref. 18). The crosses represent theoretical calculations by Klein *et al.* (Ref. 21) based on the BB potential.

Batchelder *et al.*[14] from their force-constant model, while row (f) was determined by Dorner and Egger[26] by the sound-speed method described in Sec. IV. The latter results give remarkably small values of c_{11} and c_{12} and a large positive value of δ in agreement with calculations[17] based on the BB potential with three-body forces and the zero-point energy omitted from the computation. On the basis of this agreement, Dorner and Egger concluded that solid Ar is an example of a material with only central interatomic interactions. However, the agreement between measurement and calculation obtained by Dorner and Egger must, for several reasons, be regarded as fortuitous. The measurements of Dorner and Egger are probably not particularly accurate since relatively few phonons were measured and since measurements could not be extended to wave vectors less than $q = 0.224$ Å^{-1}. In addition, no serious effort was made to correct their data for the effects of instrumental resolution. These experimental uncertainties and the fact that Dorner and Egger compared their results with a less than adequate model lead us to conclude that the agreement previously obtained between measured and calculated zero-sound elastic constants was not particularly significant. On the other hand, the present results [rows (a)–(d) of Table III], which ought to be much more reliable, do agree with the full calculation of Barker *et al.*[17] in which both three-body interaction and zero-point energy were included. Our results do not however agree with those calculated by Barron and Klein[35] from the LJ potential [row (i)] and thus one may conclude that the latter potential is less satisfactory than that proposed by Bobetic and Barker.[37]

First-sound elastic constants measured at low temperatures by Brillouin scattering[23,24] and ultrasonic[22] techniques are shown in rows (g) and (h) of Table III. Of these measurements those obtained from the ultrasonic experiments [row (h)] of Keeler and Batchelder[22] would appear to be the more reliable. While the zero- and first-sound values of c_{11} do not differ significantly there is a large discrepancy between corresponding values of c_{12} and c_{44}. The latter difference are much larger than one would expect at this temperature.[16] We can offer no explanation for this fact beyond suggesting that further ultrasonic work may serve to clarify the situation.

At 82 K the most reliable first-sound elastic constants are probably those obtained by Gewurtz *et al.*[25] [row (l) of Table III] from Brillouin scattering measurements. While the first-sound constants are consistently lower than their zero-sound counterparts obtained in our experiment, the magnitude of the difference is within the uncertainties in the measurements.

Many calculations of the elastic constants of Ar close to its melting point have been performed and the results of these are presented in rows (n)–(q) of Table III. However, the uncertainties in the experimentally determined elastic constants are not sufficiently small to allow a particular calculation to be regarded as the most reliable.

The elastic constants given in Table III have been used to determine values for the bulk modulus (B_0), elastic anisotropy (A), and deviation from the Cauchy relation (δ). These quantities are also displayed in Table III. Comparison of values of B_0, A, and δ given on different rows of the table provides little information not obtainable directly from the elastic constants. However B_0 may be compared with independent measurements of the isothermal bulk modulus B_{iso}, since this quantity can be related directly to the pressure dependence of the lattice constant. Measurements of this type have been made with x rays by Peterson *et al.*[38] and Urvas *et al.*[39] These authors found that $B_{iso} = (267 \pm 4) \times 10^8$ dyn cm^{-2} at 4 K and $B_{iso} = (127 \pm 6) \times 10^8$ dyn cm^{-2} at 78 K. Neither of these results agrees well with those obtained here in spite of the fact one would not expect a large difference between B_{iso} and the zero-sound bulk modulus at low temperatures. On the other hand, the elastic anisotropy A does follow the pattern observed in earlier neutron measurements with Kr (Refs. 8 and 9) and Xe.[10–12] At both 10 and 82 K the calculated value of δ is negative, a result which indicates[40,41] that the deviation from the Cauchy relation is a consequence of the existence of three-body forces.

A further useful test of theoretical models is provided by a comparison of observed and calculated temperature dependences of phonon energies. Unfortunately, of the experimental results displayed in Table IV only that for the [100]T mode at $\zeta = 0.4$ is directly comparable with an existing calculation.[21] A comparison for this case is displayed in Fig. 8. It is evident from this figure that the present measurements are subject to far less uncertainty than the earlier data of Batchelder *et al.*[18] While the two experiments are not completely consistent with each other they both show a more rapid variation of phonon energy with temperature than is predicted by the calculations of Klein *et al.*[21] For this reason, and in view of the additional data available in Table IV, further calculations of the temperature dependence of phonon energies in Ar would seem desirable.

For the reasons given in Sec. IV C, we are unwilling to extract from the present data any quantitative estimate of the effect of temperature on phonon linewidth. However, there can be no doubt that our measurements do demonstrate that, as temperature is increased, anharmonic broadening of the phonon profile occurs for all phonons listed in Ta-

ble IV. This is evident from an examination of Fig. 7 especially when one notes that the crystal mosaic at 75 K was *less* than that at the lower temperatures at which measurements were made. Our observation of broadening phonon profiles contradicts the result obtained by Batchelder *et al.*[18] who observed no significant increase in phonon linewidth as the temperature of the sample was increased. It is entirely plausible that this result was a consequence of the relatively poor instrumental resolution available to Batchelder *et al.*

In this experiment accurate values of phonon energies in ^{36}Ar have been measured. The use of the ^{36}Ar isotope and a high flux beam reactor have allowed excellent counting statistics to be obtained for each measured phonon profile. In addition care has been taken to avoid systematic errors in the alignment of the spectrometer. This alignment was checked by measuring the energies of phonons at equivalent points in reciprocal space and by using several values for the energy of incident neutrons. In addition some phonons were observed both via neutron-energy-loss and neutron-energy-gain processes. Finally, in order to ensure that the data are of the best possible quality, the effects of finite instrumental resolution have been taken into account in a sophisticated manner. For the above reasons we believe that the data presented here are of sufficient quality to justify further refinements of theories which describe the interatomic interactions in solid Ar.

ACKNOWLEDGMENTS

This experiment was originally conceived in cooperation with J. Skalyo, Jr. and we are indebted to him for valuable advice and assistance. We also wish to thank J. A. Barker for sending his original calculations of phonon dispersion curves of ^{36}Ar to us. Stimulating discussion with J. D. Axe is acknowledged.

---

†Work performed under the auspices of the U.S. Atomic Energy Commission.

*On leave from Institute for Solid State Physics, The University of Tokyo, Minato-ku, Tokyo 106, Japan.

‡Present address: Intelcom Rad Tech, P. O. Box 80817, San Diego, Calif. 92138.

[1]W. B. Daniels, G. Shirane, B. C. Frazer, H. Umebayashi, and J. A. Leake, Phys. Rev. Lett. 18, 548 (1967).

[2]F. P. Lipschultz, V. J. Minkiewicz, T. A. Kichens, G. Shirane, and R. Nathans, Phys. Rev. Lett. 19, 1307 (1967).

[3]V. J. Minkiewicz, T. A. Kichens, F. P. Lipschultz, R. Nathans, and G. Shirane, Phys. Rev. 174, 267 (1968).

[4]T. A. Kichens, G. Shirane, V. J. Minkiewicz, and E. B. Osgood, Phys. Rev. Lett. 29, 552 (1972).

[5]E. B. Osgood, V. J. Minkiewicz, T. A. Kichens, and G. Shirane, Phys. Rev. A 5, 1537 (1972).

[6]J. A. Leake, W. B. Daniels, J. Skalyo, Jr., B. C. Frazer, and G. Shirane, Phys. Rev. 181, 1251 (1969).

[7]J. Skalyo, Jr., V. J. Minkiewicz, G. Shirane, and W. B. Daniels, Phys. Rev. B 6, 4766 (1973).

[8]J. Skalyo, Jr. and Y. Endoh, Phys. Rev. B 7, 4670 (1972).

[9]J. Skalyo, Jr., Y. Endoh, and G. Shirane, Phys. Rev. B 9, 1797 (1974).

[10]N. A. Lurie, G. Shirane, and J. Skalyo, Jr., Phys. Rev. B 9, 2661 (1974).

[11]N. A. Lurie and J. Skalyo, Jr., Phys. Lett. A 46, 357 (1974).

[12]N. A. Lurie, G. Shirane, and J. Skalyo, Jr., Phys. Rev. B (to be published).

[13]H. Egger, M. Gsänger, E. Lüscher, and B. Dorner, Phys. Lett. A 28, 433 (1968).

[14]D. N. Batchelder, M. F. Collins, B. C. G. Haywood, and G. R. Sidey, J. Phys. C 3, 249 (1970).

[15]V. V. Goldman, S. K. Horton, T. H. Keil, and M. L. Klein, J. Phys. C 3, L33 (1970).

[16]G. Niklasson, Phys. Kondenseirten Materie 14, 138 (1972).

[17]J. A. Barker, M. L. Klein, and M. V. Bobetic, Phys. Rev. B 2, 4176 (1970).

[18]D. N. Batchelder, B. C. G. Haywood, and D. H. Sauderson, J. Phys. C 4, 910 (1971).

[19]G. K. Horton and J. W. Leech, Proc. Phys. Soc. Lond. 82, 816 (1963).

[20]G. K. Horton, V. V. Goldman, and M. L. Klein, J. Appl. Phys. 41, 5138 (1970).

[21]M. L. Klein, J. A. Barker, and T. R. Koehler, Phys. Rev. B 4, 1983 (1971).

[22]G. L. Keeler and D. N. Batchelder, J. Phys. C 3, 510 (1970).

[23]H. Meixner, P. Leiderer, and E. Lüscher, Phys. Lett. A 37, 39 (1971).

[24]H. Meixner, P. Leiderer, P. Berberich, and E. Lüscher, Phys. Lett. A 40, 257 (1972).

[25]S. Gewurtz, H. Kiefte, D. Landheer, R. A. McLaren, and B. P. Stoicheff, Phys. Rev. Lett. 29, 1768 (1972). It has recently come to our attention that Gewurtz *et al.* have refined their measurements and have obtained values of $c_{11} = (238 \pm 4) \times 10^8$ dyn cm^{-2}, $c_{12} = (156 \pm 3) \times 10^8$ dyn cm^{-2}, and $c_{44} = (112 \pm 3) \times 10^8$ dyn cm^{-2} for the elastic constants of Ar [Phys. Rev. B (to be published)].

[26]R. Dorner and H. Egger, Phys. Status Solidi 43, 611 (1971).

[27]S. A. Werner and R. Pynn, J. Appl. Phys. 42, 4736 (1971); R. Pynn and S. A. Werner, Laboratory Rept. AE-FF-112, A. B. Atomoenergi, Studsvik, Sweden (unpublished).

[28]E. C. Svensson, B. N. Brockhouse, and J. M. Rowe, Phys. Rev. 155, 619 (1967).

[29]G. Starkschall and R. G. Gordon, J. Chem. Phys. 54, 663 (1971).

[30]G. Gilat and L. J. Raubenheimer, Phys. Rev. 144, 390 (1966).

[31]P. Flubacher, A. J. Leadbetter, and J. A. Morrison, Proc. Phys. Soc. Lond. 78, 1449 (1961).

[32]R. H. Beaumont, H. Chihara, and J. A. Morrison, Proc. Phys. Soc. Lond. 78, 1462 (1961).

[33]F. Haenssler, K. Gamper, and B. Serin, J. Low. Temp. Phys. 3, 23 (1970).
[34]L. Finegold and N. E. Phillips, Phys. Rev. 177, 1383 (1969).
[35]T. H. K. Barron and M. L. Klein, Proc. Phys. Soc. Lond. 85, 533 (1965).
[36]T. H. K. Barron, in *Lattice Dynamics*, edited by R. F. Wallis (Pergamon, New York, 1965), pp. 247–254.
[37]M. V. Bobetic and J. A. Barker, Phys. Rev. B 2, 4169 (1970).
[38]O. G. Peterson, D. N. Batchelder, and R. O. Simmons, Phys. Rev. 150, 703 (1966).
[39]A. O. Urvas, D. L. Losee, and R. O. Simmons, J. Phys. Chem. Solids 28, 2269 (1967).
[40]W. Götze and H. Schmidt, Z. Phys. 192, 409 (1966).
[41]A. Hüller, W. Götze, and H. Schmidt, Z. Phys. 231, 173 (1970).